

Optimal Calibration of Qubit Detuning and Crosstalk

David Shnaiderov,¹ Matan Ben Dov,¹ Yoav Woldiger,^{1,2} Assaf Hamo,^{1,2} Eugene Demler,³ and Emanuele G. Dalla Torre¹

¹*Department of Physics, Bar-Ilan University, 52900 Ramat Gan, Israel*

²*Institute of Nanotechnology and Advanced Materials, Bar-Ilan University, 52900 Ramat Gan, Israel*

³*Institute for Theoretical Physics, ETH Zürich, 8093 Zürich, Switzerland*

Characterizing and calibrating physical qubits is essential for maintaining the performance of quantum processors. A key challenge in this process is the presence of crosstalk that complicates the estimation of individual qubit detunings. In this work, we derive optimal strategies for estimating detuning and crosstalk parameters by optimizing Ramsey interference experiments using Fisher information and the Cramér–Rao bound. We compare several calibration protocols, including measurements of a single quadrature at multiple times and of two quadratures at a single time, for a fixed number of total measurements. Our results predict that the latter approach yields the highest precision and robustness in both cases of isolated and coupled qubits. We validate experimentally our approach using a single NV center as well as superconducting transmons. Our approach enables accurate parameter extraction with significantly fewer measurements, resulting in up to a 50% reduction in calibration time while maintaining estimation accuracy.

The biggest challenge for a quantum bit is standing still. Unlike classical bits, where friction can be used to maintain the same state over time, quantum bits (qubits) are always on the move. The most common motion of an idle qubit is a random rotation around the Z axis, corresponding to a progressive randomization of the phase difference between the $|0\rangle$ and $|1\rangle$ states. To avoid this uncontrolled jitteriness, quantum computing providers need to frequently perform time-consuming calibrations on an hourly basis [1, 2]. This process delivers up-to-date values of the qubits’ rotation frequencies, or detunings, that are then used to tune the control fields used to generate quantum gates, see Refs. [3–5] for an introduction.

The process of calibrating a quantum computer is complicated by the presence of unavoidable couplings between the qubits. In particular, superconducting quantum computers are characterized by a static “crosstalk” between neighboring qubits, which changes the detuning of one qubit depending on the state of the other qubits [6–10]. Due to these terms, the calibration process cannot be performed simultaneously on all the qubits. The goal of this work is to determine the optimal strategy for calibrating single-qubit and multi-qubit systems. We will demonstrate that by carefully selecting measurement times and quadratures, it is possible to save up to 50% of the time while maintaining fixed calibration precision.

To introduce our optimal strategy, we first consider the case of a single qubit, whose detuning ω is unknown. To mimic realistic conditions, we assume that the qubit undergoes a dephasing process. The dynamics of the qubit are then described by

$$H = \frac{\omega}{2}(1 - Z) + h(t)(1 - Z). \quad (1)$$

Here, Z is a Pauli matrix with eigenvalues $+1$ and -1 , respectively for the $|0\rangle$ and $|1\rangle$ states, and $h(t)$ is a Gaussian random process with $\langle h(t) \rangle = 0$ and two-point cor-

relation function $\langle h(t)h(t') \rangle = F(t - t')$ [11–13].

The common procedure to calibrate the qubit consists of a series of Ramsey interference experiment, where (i) an initial $\pi/2$ pulse prepares the qubit in the superposition state, $|+\rangle = (|0\rangle + |1\rangle)/\sqrt{2}$; (ii) the qubit is let evolve freely for time t ; and (iii) the Pauli operator X is measured by applying a second $\pi/2$ pulse and measuring the qubit in the computational basis. The experiment is repeated for varying t and the average result is stored as $\langle X(t) \rangle_{\text{exp}}$. This quantity is then compared to the theoretical result obtained by evolving the initial state with Eq. (1), $|\psi\rangle = [|0\rangle + \exp(-i\omega t - i \int_0^t dt' h(t')) |1\rangle] / \sqrt{2}$ and averaging over $h(t)$, leading to $\langle X(t) \rangle_{\text{theory}} = \cos(\omega t) \exp\left(-\frac{1}{2} \int_0^t dt' \int_0^t dt'' F(t' - t'')\right)$. If the noise correlations have short memory, one can approximate $F(t - t') = \gamma \delta(t - t')$, where γ is the dephasing rate and $\delta(t - t')$ is the Kronecker delta. In this case, often referred to as the Markovian limit, one obtains a closed expression that depends on ω and γ only

$$\langle X(t) \rangle_{\text{theory}} = \cos(\omega t) e^{-\gamma t} \quad (2)$$

These two parameters are then estimated by minimizing the difference between $\langle X(t) \rangle_{\text{exp}}$ and $\langle X(t) \rangle_{\text{theory}}$ [14]. In the case of a noise bath with a correlation time τ_{bath} comparable to $1/\gamma$, it is possible to derive an analytic expression that depends on both τ_{bath} and γ [15] and can be easily incorporated in the present approach.

In a real experiment, the precision of the above-mentioned procedure is limited by different sources of noise, such as state preparation and measurement (SPAM) errors, imperfections in the $\pi/2$ pulses, and shot noise. The former two types of noise do not depend on the number of measurement times, N_{times} , and, for state-of-the-art quantum computers with single-qubit gate fidelity of 99.9%, limit the calibration precision to about

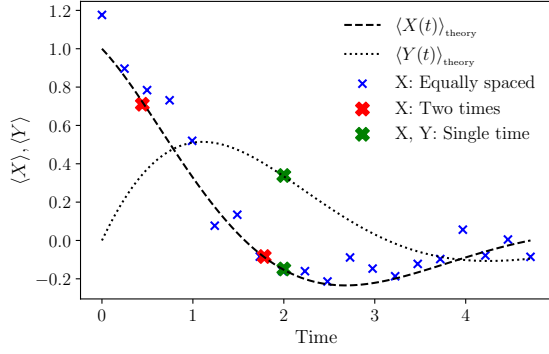


FIG. 1. Three strategies to calibrate the frequency ω and dephasing rate γ of a single qubit, respectively denoted by blue, red, and green crosses, see text for details. The blue strategy is noisier because it uses more measurement times with fewer shots in each of them.

10^{-3} or less. The latter source of noise refers to the fact that each individual measurement (or, *shot*) of $X(t)$ returns $+1$ and -1 and leads to a standard deviation that scales with $1/\sqrt{N_{\text{shots}}}$. For a given total number of shots $N_{\text{tot}} = N_{\text{times}} N_{\text{shots}}$, one should allocate this resource wisely among the different measurement times. A fundamental question that we address is whether one obtains a better precision by performing many measurements at fewer times (see red crosses in Fig. 1 for $N_{\text{times}} = 2$ and $N_{\text{shots}} = 1000$), or on the contrary, by spreading the measurements over a larger number of times (see blue crosses in Fig. 1 for $N_{\text{times}} = 20$ and $N_{\text{shots}} = 100$).

Here, we address this question using the Cramér-Rao bound, which sets the theoretical lower limit on the variance of any unbiased estimator. The Cramér-Rao bound is the inverse of the Fisher information [16], \mathcal{I} , which quantifies how much information a set of measurements provides about an unknown parameter of interest. For a set of variables \mathbf{X} whose probability distribution $f(\mathbf{X}|\boldsymbol{\theta})$ depends on a set of parameters $\boldsymbol{\theta}$, \mathcal{I} is defined as

$$\mathcal{I}_{jk}(\boldsymbol{\theta}) = \mathbb{E}_{\mathbf{X}} \left[\frac{\partial}{\partial \theta_j} \ln L(\boldsymbol{\theta}|\mathbf{X}) \frac{\partial}{\partial \theta_k} \ln L(\boldsymbol{\theta}|\mathbf{X}) \right], \quad (3)$$

where $L(\boldsymbol{\theta}|\mathbf{X}) = f(\mathbf{X}|\boldsymbol{\theta})$ is the likelihood function and $\mathbb{E}_{\mathbf{X}}$ is the weighted average over \mathbf{X} . The Cramér-Rao bound states that the covariance of an unbiased estimator $\hat{\boldsymbol{\theta}}$ is bounded from below by the inverse of the Fisher information matrix and can be formally expressed as

$$\text{cov}(\hat{\boldsymbol{\theta}}) \geq \mathcal{I}^{-1}. \quad (4)$$

In the problem at hand, $\boldsymbol{\theta} = (\omega, \gamma, t_1, t_2, \dots, t_{N_{\text{times}}})$, $\mathbf{X} = (X_1, X_2, \dots, X_{N_{\text{times}}})$, and X_i is the average of N_{shots} binary, independent measurement outcomes with mean value $\langle X(t) \rangle$, given in Eq. (2). Here, for simplicity, we assume that each measurement time is probed with the same number of shots N_{shots} . See SM1 for the generic

case of $N_{\text{shots},i} \neq N_{\text{shots}}$. In the limit of a large number of measurements $N_{\text{shots}} \gg 1$, the Fisher information can be further simplified by applying the central limit theorem and assuming that X_i is sampled from a normal distribution. In this limit (see SM2 for a derivation), the Fisher information matrix simplifies to

$$\mathcal{I}_{jk}(\boldsymbol{\theta}) = N_{\text{shots}} \sum_{n=1}^{N_{\text{times}}} \frac{\partial \langle X(t_n) \rangle}{\partial \theta_j} \frac{\partial \langle X(t_n) \rangle}{\partial \theta_k} \quad (5)$$

According to Eq. 5, the Fisher information matrix corresponds to the products of the sensitivity of the observables to changes in two parameters.

In this work, we aim to optimize the calibration strategy by *minimizing* the sum of the Cramér-Rao bound for each parameter, i.e. by minimizing $\text{Tr}[\mathcal{I}^{-1}(\boldsymbol{\theta})]$. A similar approach was introduced in the context of NMR experiments [17] to find the optimal times used to probe the function $Ae^{-\gamma t}$, where A and γ are fitting parameters. It was numerically found that the optimal strategy involves probing the function at times $t = 0$ and $t \approx 1.1/\gamma$. By applying this approach to the guess function Eq. (2), we recover a similar result: the optimal strategy involves measuring only two times. The optimal times depend on ω and γ and can be found numerically (see SM1 for details about the optimization procedure). In what follows we focus on the case of $\omega = \gamma$, where the optimal times are $t_1 \approx 0.4439/\gamma$ and $t_2 \approx 1.7846/\gamma$.

Unlike NMR experiments, qubit calibration involves a finite-frequency rotation around the z axis, ω . This observation suggests that qubit calibration may be improved by measuring two quadratures of the qubit: by adding a $\pi/2$ phase to the second pulse one can effectively measure $Y(t)$, whose theoretical expectation value is $\langle Y(t) \rangle = \sin(\omega t)e^{-\gamma t}$. Importantly, such a modification comes “for free” as it simply corresponds to a constant shift in the carrier signal of the second pulse and is not expected to add additional noise. By optimizing the Fisher information, we find that the optimal strategy consists of measuring $X(t)$ and $Y(t)$ at a single time $t = 1/\gamma$, which is remarkably independent of ω , see SM3 for a derivation. With respect to the common approach, this strategy leads to a reduction of the Cramér-Rao bound of approximately 0.7, corresponding to a $0.7^2 \approx 50\%$ reduction in the number of shots for a given precision. In addition, because $\langle Y(t) \rangle$ is anti-symmetric with respect to ω , one can determine both the amplitude and the sign of ω , while the latter is inaccessible by X measurements only.

To validate our optimization procedure, we now compare the theoretical bound with numerical simulations of the model: We compute the time-dependent density matrix describing the noise-averaged evolution under the Hamiltonian (1) by solving the corresponding Lindblad master equations using the QuTiP Python library [18].

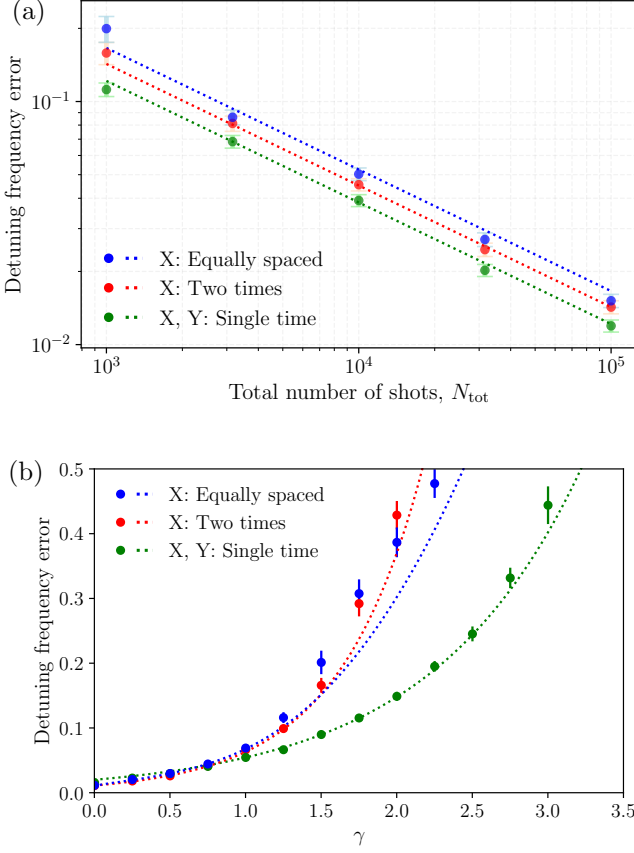


FIG. 2. Numerical simulation of three strategies for estimating the qubit detuning and dephasing rate as a function of (a) the total number of shots, $N_{\text{tot}} = N_{\text{times}} N_{\text{shots}}$, (b) actual dephasing rate (see text for details). The circles are numerical results, and the dotted lines are the Cramer-Rao bound. The optimal strategy (green) involves measuring X and Y simultaneously at $t = 1/\gamma$.

The effect of shot noise is introduced by drawing samples from the resulting density matrix [19]. We use the noisy numerical result to compute $\langle X(t) \rangle_{\text{noisy}}$ and fit it to Eq. (2) by minimizing the mean-square error (MSE) between the two curves. The extracted γ_{noisy} and ω_{noisy} are then compared to the theoretical value.

Typical results from this approach are shown in Fig. 2 (a), where we chose $\omega = \gamma = 1$. This figure shows the relative root mean-square errors (RMSE) of the the detuning frequency, $[\mathbb{E}(\omega_{\text{noisy}} - \omega)^2]^{1/2}/\omega$, as a function of N_{tot} , for three different approaches: the measurement of $X(t)$ for $N_{\text{times}} = 20$ equally spaced times; the measurement of $X(t)$ the two optimal times computed using the Fisher information; the measurement of $X(t)$ and $Y(t)$ at a single time. All the plots follow the expected $1/\sqrt{N_{\text{tot}}}$ shot-noise dependence. The circles are the result of numerical simulations, and the dashed lines are the analytical results for the Cramer-Rao bound obtained by solving Eq. (5). The two approaches are in perfect agree-

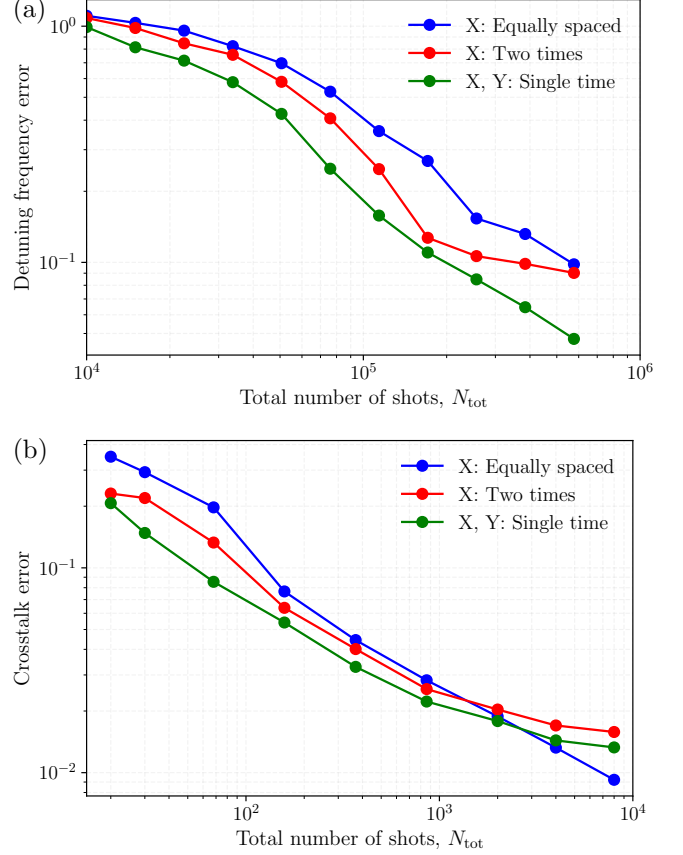


FIG. 3. Experimental comparison of three different strategies to calibrate (a) the detuning a single NV center qubit; (b) the crosstalk between two superconducting qubits. In both cases, measuring two quadratures at the same time converges fastest as a function of number of shots, reducing the error significantly and systematically.

ment and demonstrate that the third method is superior to the other two methods.

The approach described so far has a “catch-22” problem: the optimal times that we computed required the knowledge of ω and γ , which are the parameters that we are trying to optimize. To address this problem, we assume that the detuning and decay rates change slowly over time, such that one can use their earlier values to obtain an estimate, albeit not exact, of their current values. In this scenario, we need to check the resilience of the different methods to variation in the actual value of ω and γ . This analysis is performed in Fig. 2(b), where we vary γ , while keeping fixed the measurement times. We, again, find that the third method (measuring X and Y at the same time) is the least sensitive to variations of γ . A similar conclusion can be drawn for the stability to variations of ω .

We conclude the analysis of the single-qubit case by describing the results of an experiment using a single NV center. The experimental results of a Ramsey in-

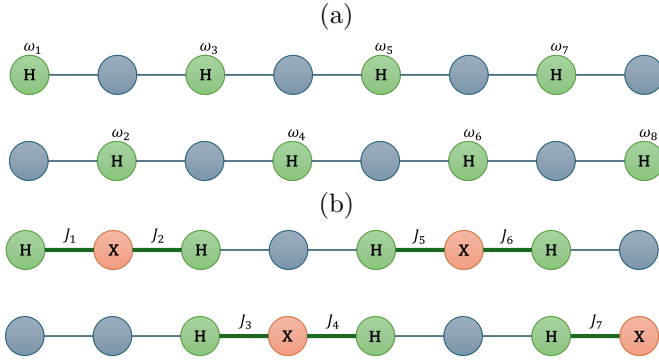


FIG. 4. Schematic representation of the four experiments used to calibrate the multi-qubit system defined in Eq. (6): (a) two experiments are used to measure ω_j : the green nodes represent qubits in the $|+\rangle$ state, and the blue nodes represent qubits in the $|0\rangle$ state; (b) two experiments are used to measure J_j : the red nodes represent qubits in the $|1\rangle$, the green nodes represent qubits in the $|+\rangle$ state, and the blue nodes represent qubits in the $|0\rangle$ state. The green edges are the measured crosstalk.

interference experiment were fit using the curves $X(t) = A \cos(\omega t + \phi) e^{-\gamma t} + B$. We first determined the “ground truth” values of all parameters using a long measurement with $N_{\text{shots}} = 10^5$ and $N_{\text{times}} = 100$. Next, to allow a direct comparison between the three strategies reported here, we fixed A , B and ϕ to their “true” values and determined ω and γ from a random downsampling of the experimental measurements, with up to $N_{\text{tot}} = 5 \times 10^5$. Alternatively, one could extend our approach by using the Fisher Information to find the optimal strategy to probe all five fitting parameters. The experimental results, shown in Fig. 3 confirm our theoretical predictions for the comparison between the three strategies [20].

We now move to the systems of coupled qubits relevant to quantum computers. We consider a canonical model describing the interactions between qubits as a static crosstalk ZZ term [6–10]. For simplicity, we consider a one-dimensional chain described by

$$H = \sum_{i=1}^{N_{\text{qubits}}} \left[\frac{\omega_i}{2} + h_i(t) \right] (1 - Z_i) + \frac{J_i}{4} (1 - Z_i)(1 - Z_{i+1}) \quad (6)$$

The crosstalk couplings J_i effectively shift the frequency of the i th qubit if the $i+1$ th qubit is in the $|1\rangle$ ($Z_{i+1} = -1$) state, and vice versa. Importantly, Eq. (6) is diagonal in the Z basis and can be solved analytically for any initial state.

A naive approach to the problem of calibrating the system described by Eq. (6) consists of preparing all qubits in the $|+\rangle$ state and performing simultaneous Ramsey interference experiments. By fitting the resulting $X_i(t)$ and $Y_i(t)$ to the theoretical curves, one can estimate all the parameters. While this approach is formally correct, we

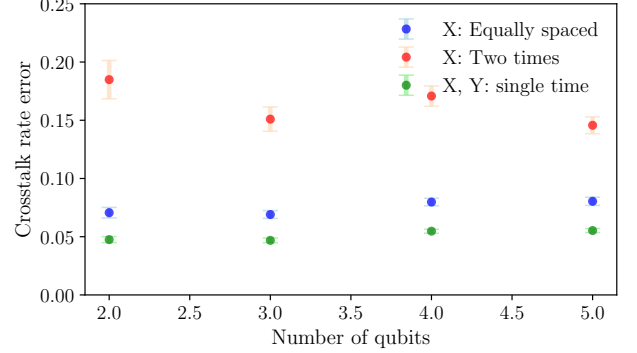


FIG. 5. Numerical simulation of crosstalk-rate error as a function of the number of qubits. The parameters were sampled from a normal distribution $\omega, \gamma \in N(1, 0.2)$, $J \in N(0.5, 1)$. The simulation used the protocols described in fig. 4.

found that it is not optimal, due to the complex shape of the resulting analytical functions, and generically leads to errors that are one order of magnitude larger than the optimal ones, see SM4.

Our proposed strategy for computing the values of ω_i and J_i involves reducing the many-body problem to that of isolated single qubits. Specifically, we propose to perform two pairs of experiments, respectively, to probe the detunings and the crosstalk couplings, see Fig. 4 for details. Each experiment involves a Ramsey interference experiment on half of the qubits (denoted by “H”), for different initial states of the other qubits. In the former two experiments, the qubits rotate at frequency ω_i , while in the latter two, they rotate at frequency $\omega_i + J_{i\pm 1}$. The numerical results of this approach are presented in Fig. 5 and demonstrate the scalability of our protocol, as the error is essentially independent of the system size. Measuring X and Y simultaneously is optimal in this problem as well.

This approach can be straightforwardly extended to quantum computers with a more complex connectivity between the qubits. In general, the number of experiments needed to calibrate the system depend on the amount on non-negligible crosstalk couplings per qubit. For bipartite lattices with nearest-neighbor couplings, it is easy to see that one can determine all the systems’ parameters using the same four experiments as in the one-dimensional case. Interestingly, for IBM’s heavy-hex topology, one can show that four experiments are sufficient as well, see SM5. For more complex topologies, the problem at hand can be formulated as a tiling optimization problem, which can be solved heuristically and warrants further investigation.

We demonstrated the feasibility of this approach by calibrating the crosstalk coupling between two transmon qubits in the Gilboa superconducting quantum computer [21], with up to $N_{\text{times}} = 30$ and $N_{\text{shots}} = 20000$. The experimental results are shown in shown Fig. 3(b) and

demonstrate two separate regimes: for $N_{\text{tot}} < 10^3$, the curves follow our theoretical modelling, while for larger N_{tot} measurements based on one or two times saturate to a value that is different than the one obtained by using all measurement times. This discrepancy indicates that the experiment deviates from our simple-minded theoretical model and can be fixed by considering more realistic theoretical models, for example, affected by quasiparticle fluctuations [22, 23], which go beyond the scope of the present analysis.

In summary, this article proposes and validates optimal strategies for characterizing qubit detuning and crosstalk in superconducting quantum computers. While traditional methods spread measurements across multiple times to average out noise, our work demonstrates that concentrated, optimally-timed measurements can achieve better results with fewer resources. By analyzing different measurement protocols using the Fisher information framework and the Cramer–Rao bound, we demonstrated that simultaneous measurement of both X and Y quadratures at a single optimal time yields the best precision and resilience to parameter variation. We then extended our analysis to multi-qubit systems, where we described a method that effectively reduces the estimation of crosstalk terms to decoupled single-qubit problems, drastically simplifying calibration. Our framework scales well to larger systems and complex architectures, making it highly relevant for current and future quantum processors. Experimental validation and simulations confirm that the proposed strategies can cut calibration time by up to 50% without compromising accuracy. Looking forward, integrating these optimized calibration strategies into real-time control systems could significantly enhance the stability and scalability of quantum computing platforms.

Acknowledgments We acknowledge useful discussions with O. Hamdi and S. Burov. We are thankful to N. Alfasi and O. Ovdatt from the Israeli Quantum Computing Center (IQCC) for technical support. D.S. and E.G.D.T. are supported by the Israel Science Foundation, grants No. 2126/24 and 2471/24.

[1] IBM Quantum Administration. About calibration jobs. URL <https://docs.quantum.ibm.com/admin/calibration-jobs>.
 [2] Google Quantum, Rigetti Computing, IQCC, and others. Private communications.
 [3] Siddiqi, I. Engineering high-coherence superconducting qubits. *Nature Reviews Materials* **6**, 875–891 (2021).
 [4] Chatterjee, A. *et al.* Semiconductor qubits in practice. *Nature Reviews Physics* **3**, 157–177 (2021).
 [5] Kjaergaard, M. *et al.* Superconducting qubits: Current state of play. *Annual Review of Condensed Matter Physics* **11**, 369–395 (2020).
 [6] Mundada, P., Zhang, G., Hazard, T. & Houck, A. Sup-

pression of qubit crosstalk in a tunable coupling superconducting circuit. *Physical Review Applied* **12**, 054023 (2019).
 [7] Ni, Z. *et al.* Scalable method for eliminating residual zz interaction between superconducting qubits. *Physical review letters* **129**, 040502 (2022).
 [8] Xie, L. *et al.* Suppressing zz crosstalk of quantum computers through pulse and scheduling co-optimization. In *Proceedings of the 27th ACM International Conference on Architectural Support for Programming Languages and Operating Systems*, 499–513 (2022).
 [9] Heng, S., Go, M. & Han, Y. Estimating the effect of crosstalk error on circuit fidelity using noisy intermediate-scale quantum devices. *arXiv preprint arXiv:2402.06952* (2024).
 [10] Fors, S. P., Fernández-Pendás, J. & Kockum, A. F. Comprehensive explanation of zz coupling in superconducting qubits. *arXiv preprint arXiv:2408.15402* (2024).
 [11] Breuer, H.-P. & Petruccione, F. *The theory of open quantum systems* (OUP Oxford, 2002).
 [12] Benedetti, C. & Paris, M. G. Effective dephasing for a qubit interacting with a transverse classical field. *International Journal of Quantum Information* **12**, 1461004 (2014).
 [13] Shirizly, L., Misguich, G. & Landa, H. Dissipative dynamics of graph-state stabilizers with superconducting qubits. *Physical Review Letters* **132**, 010601 (2024).
 [14] Qiskit community. T2* ramsey characterization. URL <https://qiskit-community.github.io/qiskit-experiments/manuals/characterization/t2ramsey.html>.
 [15] Curtis, J. B., Yacoby, A. & Demler, E. Non-gaussian noise magnetometry using local spin qubits. *arXiv preprint arXiv:2505.03877* (2025).
 [16] Ly, A., Marsman, M., Verhagen, J., Grasman, R. P. & Wagenmakers, E.-J. A tutorial on fisher information. *Journal of Mathematical Psychology* **80**, 40–55 (2017).
 [17] Jones, J., Hodgkinson, P., Barker, A. & Hore, P. Optimal sampling strategies for the measurement of spin–spin relaxation times. *Journal of Magnetic Resonance, Series B* **113**, 25–34 (1996).
 [18] Johansson, J. R., Nation, P. D. & Nori, F. Qutip: An open-source python framework for the dynamics of open quantum systems. *Computer physics communications* **183**, 1760–1772 (2012).
 [19] Grynberg, G., Aspect, A. & Fabre, C. *Introduction to quantum optics: from the semi-classical approach to quantized light* (Cambridge university press, 2010).
 [20] Note that the experimental measurements are of statistical nature as (i) they rely on a weak spin-dependent fluorescence difference of about 30% and (ii) the collection efficiency of photons is approximately 10%. These two effects explain the vertical shift of almost two orders of magnitude between theory and experiment.
 [21] Israel Quantum Computing Center. The future of high-performance quantum computing (2025). URL <https://i-qcc.com/>.
 [22] Serniak, K. *et al.* Hot nonequilibrium quasiparticles in transmon qubits. *Physical review letters* **121**, 157701 (2018).
 [23] Landa, H. & Misguich, G. Nonlocal correlations in noisy multiqubit systems simulated using matrix product operators. *SciPost Physics Core* **6**, 037 (2023).